Check for
updates

Measuring chloride binding in cementitious materials: A review by RILEM TC 298-EBD

Fabien Georget · **Arezou Babaahmadi** · **Alisa Machner** · **Maruša Mrak** ·
Sabina Dolenec · **Qing Xiang Xiong** · **Joseph Shiju** · **Didier Snoeck** ·
Prannoy Suraneni · **William Wilson**

Abstract The phase assemblage evolution of binders with novel supplementary cementitious materials (SCM$_S$) during exposure to adverse environments needs to be quantified to accelerate their adoption, and further optimize binder formulation. As such, the interaction between chloride and cementitious matrices with novel SCMs needs to be quantified. The goal of workgroup 2 of RILEM TC EBD-298 is to assess the methods used to quantify chloride binding. This state-of-the-art report reviews the standardized and novel methods to measure chloride binding through an average content (acid/water soluble) or a specific bound content per phase (XRD, TGA, SEM–EDS, …). Each method is presented with respect to our current understanding of chloride binding and speciation in cementitious materials. The discussion around the purpose, use and reporting of each method highlights the gaps limiting the comparison between studies, in particular the lack of standard protocol, and complementary characterization. This review is

F. Georget (✉)
Institute of Building Materials Research, RWTH Aachen University, Aachen, Germany
e-mail: fabien.georget@usherbrooke.ca

F. Georget · W. Wilson
Department of Civil and Building Engineering, Université de Sherbrooke, Sherbrooke, Canada
e-mail: william.wilson@usherbrooke.ca

A. Babaahmadi
Department of Architecture and Civil Engineering, Chalmers University of Technology, Gothenburg, Sweden
e-mail: arezou.ahmadi@chalmers.se

A. Machner
Professorship for Mineral Construction Materials, TUM School of Engineering and Design, Technical University Munich, Munich, Germany
e-mail: alisa.machner@tum.de

the groundwork for a "cookbook" of experimental workflows to investigate chloride binding in modern cementitious binders.

1 Introduction

The introduction of new binders and novel supplementary cementitious materials (SCMs) to mitigate climate change is slowed by the necessity to provide safe and durable infrastructure, and living environment. It is a challenge as we lack the necessary real-world experience to assess the potential to achieve the long-term resistance of these new materials to durability issues. In particular, chloride ingress is one of the main durability issues for reinforced concrete [1]. Although it was shown that quantifying corrosion is crucial to predict the loss of mechanical properties [2], the effect of the binder needs to be understood with respect to its chemistry and its interaction with chloride, so that safe and durable mixture designs can be used in practice [3].

Extensive research has been carried out on chloride binding in cementitious materials (e.g. [4–13]), but we are still far from being able to predict the impact of a binder on the chloride binding capacity of a concrete [3, 14]. The binding capacity is the ability of the cementitious matrix to bind chloride to its solid phases. There are usually two main mechanisms of chloride binding identified in the literature: chemical and physical binding. The chemical binding is the

inclusion of chloride atoms in the structure of a solid phase. The main cementitious hydrates able to chemically bind chloride are members of the AFm family: $[Ca_2(Al,Fe)(OH)_6]\cdot X\cdot yH_2O$, where X represents a monovalent ion (e.g., OH^-, Cl^-), or half of a divalent interlayer anion, (e.g., $0.5\ SO_4^{2-}$, $0.5\ CO_3^{2-}$), and y represents the number of water molecules. Chloride incorporation in the AFm phases leads to the formation of Friedel's salt, or associated solid phases [15]. Although chloride incorporation in these phases is a well-known mechanism, there are still many open questions, and no thermodynamic model correctly represents Friedel's salt solid solutions [16]. Chemical binding is also reported for hydrotalcite: $Mg_6Al_2CO_3(OH)_{16}\cdot4H2O$ [10, 17]. In addition, it leads to the formation of calcium oxychloride at high chloride content ($\sim 15\%\ CaCl_2$) and low temperature [18]. On the other hand, physical binding is the sorption of chloride on the surface of a solid phase. The main known contributor to this mechanism is the calcium silicate hydrate phase (C–S–H). Some models exist [8, 19] although their application or validation to a wide range of systems is still under discussion [12, 20], notably because a generic C–S–H model is still missing [21].

Most of the issues with modeling chloride binding come from the challenge to quantify them in situ [14]. The binding isotherm is a tool often used in many scientific fields to quantify the fraction of the species uptake by the solid as a function of the concentration of the species in the equilibrium solution. It is also often used for cementitious materials as represented in Fig. 1. As highlighted in the previous paragraph, the total chloride binding can be separated into several contributions. However, standard measurement

M. Mrak · S. Dolenec
Slovenian National Building and Civil Engineering Institute, Ljubljana, Slovenia
e-mail: marusa.mrak@zag.si

S. Dolenec
e-mail: sabina.dolenec@zag.si

S. Dolenec
Department of Geology, Faculty of Natural Sciences and Engineering, University of Ljubljana, Ljubljana, Slovenia

Q. X. Xiong
Shanghai Jiao Tong University, Shanghai, China
e-mail: qingxiangxiong@sjtu.edu.cn

J. Shiju
Department of Engineering, University of Cambridge, Cambridge, UK
e-mail: sj685@eng.cam.ac.uk

D. Snoeck
BATIr Department, Université Libre de Bruxelles (ULB), Brussels, Belgium
e-mail: didier.snoeck@ulb.be

P. Suraneni
Civil and Architectural Engineering, University of Miami, Coral Gables, FL, USA
e-mail: suranenip@miami.edu
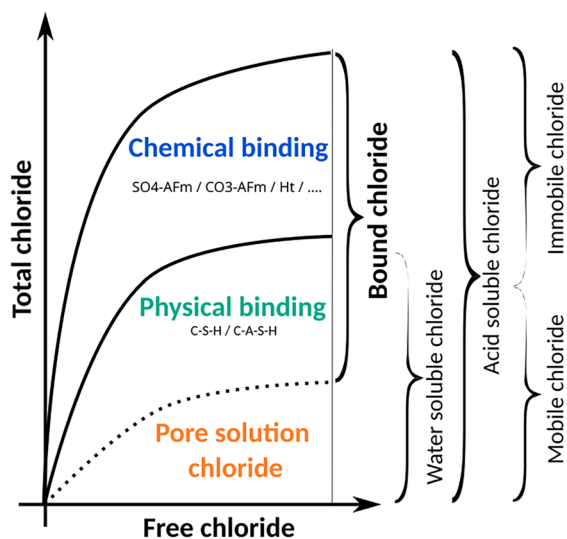
Fig. 1 Schematic representation of a typical chloride binding isotherm and its classification in different classes of chloride species

methods only provide two data points provided by the acid-soluble [22] and water-soluble methods [23], which are assumed to provide the total chloride content and the free chloride content, respectively. However, there are no standardized methods to analyze the individual binding mechanisms, and the interpretation of acid and water-soluble chloride interpretation is under debate [13, 20]. A new classification of chlorides as mobile and immobile chloride was proposed recently [3] as these classes better suit the needs of modelers but their correlation to the physical classes of chloride is not straightforward due to the lack of generic thermodynamic models to predict the chloride binding isotherm [3, 14], as well as the issue of interpretation of what chloride mobility actually means in C–S–H gel pores [3, 24, 25].

To better predict the impact of novel binders on binding isotherms, it is necessary to better quantify the contribution of each phase to the overall binding. This is widely recognized in the literature and many advancements have been made in the last decades [3, 9, 13, 20, 26–28]. Thus, the goal of this article is to review these advances in the field of chloride binding, with a particular focus on the measurement methods. We review each method which allows to describe the different classes of chloride highlighted in Fig. 1, in terms of a few governing questions:

What is measured? How is it measured? How well is it measured? We also provide a few representative studies for the use of these methods to demonstrate how the complementary information obtained by the combination of these methods can be used to improve our understanding of chloride binding mechanisms and their quantification. This review will be used by TC 298-EBD to justify a set of recommendations on which methods and protocols to use as function of the goal of the investigation.

2 Bulk methods

2.1 Measuring chloride in solution

Many bulk methods rely on measuring the chloride in solution after equilibrium with the solid phases, extraction of bound chloride in acid/water solution, or after dissolution of the solid phases in a solution. As such, these methods rely on the accurate determination of the chloride concentration in solution.

2.1.1 Titration

Various methods for titration have been adopted for determining the chloride content in a solution. Among them, potentiometric and Volhard methods are most commonly applied.

The potentiometric titration method as used in AASHTO T 260–21 [29] or ASTM C1152 [22] involves titrating a chloride solution with an $AgNO_3$ solution. The equivalence point, i.e. the amount of added $AgNO_3$ solution corresponding to the highest electric potential change, is used to determine the chloride concentration in solution. The electric potential is measuring with either a Cl^- or Ag^+ electrode.

The Volhard titration method is a back-titration method. It is used for example in the Nordic standard NT BUILD 208 [30]. First, an excess 0.1 M $AgNO_3$, along with 2 to 3 ml of benzyl alcohol or nonanol and 1 ml of saturated ammonium ferri-sulfate, are introduced. The final step is colorimetric titration using 0.1 M ammonium thicyanate (NH_4SCN).

The choice of these methods mainly depends on locally accepted norms regarding the accuracy or reproducibility offered by each method, as well as the familiarity of the lab with each method. Tang [31] studied the performance of two titration methods for

OPC as well as fly ash, slag, and silica fume-substituted concrete across four different laboratories. The study found that both methods have limitations in accurately determining chloride content within the range of 0.4–0.5% Cl by mass of binder. The potentiometric titration method tends to underestimate chloride content by 1.5–3% for OPC and silica fume-blended concrete and by 7–9% for slag or fly ash-blended concrete. The Volhard titration method also underestimates chloride content but to a greater extent, approximately 8% for OPC and silica fume-blended concrete and around 18% for slag or fly ash-blended concrete. Due to these discrepancies, Tang suggests that the Volhard titration method requires modification when testing samples with lower chloride content to achieve acceptable repeatability and reproducibility. However, for samples with higher chloride content (> 0.05% Cl by mass of sample), the Volhard titration method has shown to provide satisfactory repeatability and reproducibility. The recommendation from Nordtest (NT BUILD 208 [30]) concludes that the potentiometric method is more accurate among the two different types of titration methods [30]. Similarly, Potgieter et al. compared the Volhard and potentiometric titrations for South African cement, clinker and raw materials, and found that the superior method of analysis proved to be an acetic acid dissolution followed by a potentiometric titration [32].

On the other hand, a study conducted on the determination of total chloride content in reinforced concrete, undertaken by RILEM TC 178-TMC comprising 30 different laboratories around the world, recommended the Volhard method as most suitable for calculating the total chloride content [33]. Their procedure for analyzing the total chloride content is divided into extraction and quantification followed by an estimation of the reliability of these two steps individually. However, it is worth pointing out that in this study, the Volhard titration method was utilized by a significantly smaller number of laboratories compared to the Potentiometric titration method. This observation suggests that there may be fewer technical facilities equipped with the expertise required for performing the Volhard method.

2.1.2 IC and ICP-OES

Ion Chromatography (IC) or Inductively Coupled Plasma with Optical Emission Spectroscopy (ICP-OES) belong to the classical wet chemistry analyses of solutions. As a chromatographic method, IC is a two-step method. First, the species are separated, then quantified [34]. For the separation, the liquid sample needs to move through a separation column that contains a so-called stationary phase and is flushed by a so-called mobile phase. The liquid sample is injected into the mobile phase (e.g., carbonate solution). The injected sample then interacts with the stationary phase (e.g. plastic material combined with quaternary amino groups), which leads to a retarded ion transport through the separation column [35]. Depending on the type of ion, they interact more or less with the stationary phase, so different ions require different times to reach the other end of the separation column, thereby, various ions are separated by retention time. At the end of the column, a detector is placed. For anion determination, a conductivity measurement is commonly used [36].

The ICP-OES belongs to the optical, more specifically, the spectroscopic methods. It relies on the inelastic interaction (energy conversion) of the sample with electromagnetic radiation. In the ICP part of the method, the sample is atomized, ionized, and excited by a hot Argon plasma. The excited ions then relax into ground states again, emitting electromagnetic radiation of an element-specific wavelength. This radiation can then be detected and quantified by the optical spectroscopy part of the method. Commonly, wavelengths in or near the visible light spectrum between 160 and 900 nm are measured by ICP-OES [37, 38].

Due to their differences in measurement principles, both methods show different quantification limits [39]. While the ICP-OES generally is a reliable and accurate measurement method [37], the quantification of chloride is rather complicated with this method. This is because the emission band of chlorine at 837.6 nm is rather weak, and the signal from an additional emission band at 134.7 nm is absorbed by air and can only be detected by the use of special optics [40–42]. In nitric acid matrices, the reported limit of detection (LOD) is 50–120 µg/L [43, 44]. For chloride analyses, IC shows considerably better LOD. In drinking water analysis, a common method detection

Fig. 2 Comparison of chloride profiles determined from titration and μXRF after chloride ponding for **a** 45 days, **b** 90 days and **c** 135 days (reproduced with permissions from [28]). μXRF-reduced data points are obtained by averaging the profile over the depth
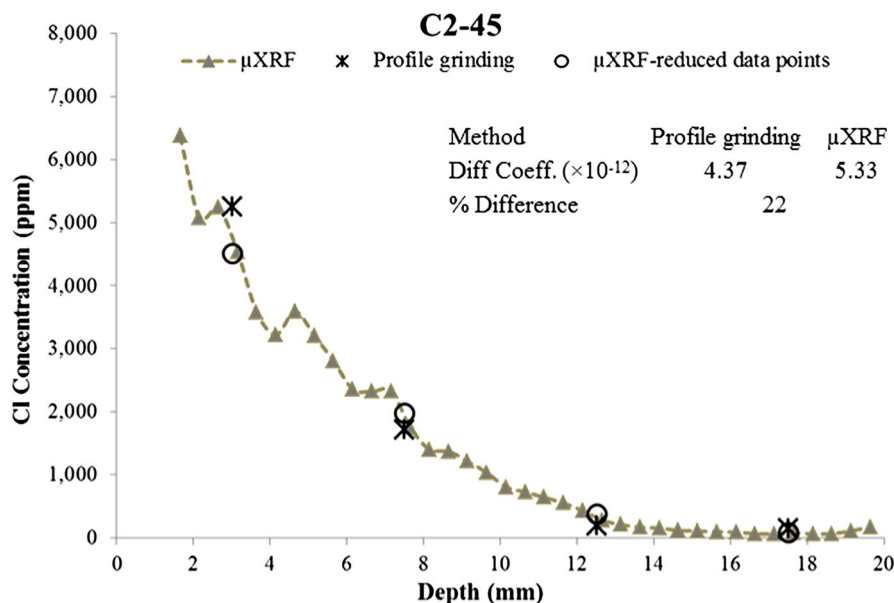
limit (MDL) is 5 μg/L. In samples of 0.5 g extracted with 100 mL deionized water, this translates to a mass concentration of approx. 0.0001 wt.% [45]. However, since the samples of interest are commonly extracted from concrete samples, they show a high concentration of other ions as well (e.g. NO_3^- from extraction in nitric acid, or SO_4^{2-}, Na^+, K^+, and Ca^{2+}). Thus, the samples need to be considerably diluted before being measured.

UV/Visible and near-infrared spectrometry has also been used to measure chloride concentration in solution [46–48]. However, to the authors' knowledge, the use of these methods in routine measurements in concrete applications is not reported in the scientific literature.

For these reasons, titration methods, and potentiometric methods in particular, are usually regarded as the "go-to" methods in the literature, due to their shorter time, lower equipment and expertise requirements.

2.2 Measuring chloride in solids

Although, chloride determination from solution is a common method, there is some interest to measure chloride content directly from the solid to accelerate the process. Micro-X-Ray Fluorescence (μXRF) is a relatively recent addition to characterize the chloride profile of concrete, and by extension the chloride

binding in-situ. This technique is a method for elemental analysis which involves the use of X-rays to stimulate the atoms within the sample. This prompts the atoms to emit X-rays with distinct energy signatures which are used to identify and quantify the individual elements in the sample. μXRF is well suited to measure the average elemental distribution as the interaction volume is significantly larger than the characteristic size of cement paste phases (spot size of 20–50 μm). The measurement can be carried out at selected point on a cross-section to obtain a concentration profile.

μXRF provides energy spectra and chloride counts, which can be quantified (if needed) with calibration curves obtained for similar cementitious samples doped with known amounts of chloride [49]. The limit of detection and the limit of quantification were determined to be about 0.003 and 0.011 w% of cement respectively [49]. This is on par with the titration method to determine the total chloride content (Sect. 2.3.2). Figure 2 shows a comparison between chloride profiles determined from μXRF and total acid soluble chloride from titration. A good correlation is generally found between depth-averaged μXRF measurements and acid titration [28, 50]. Calibration with doped samples requires more efforts and is required for the quantification of chloride binding. However, chloride counts (with specific instrument parameters) readily provide a strong comparative

basis for analyzing chloride profiles and chloride ingress (e.g., with penetration depths) [51].

Laser-Induced Breakdown Spectroscopy (LIBS) is another method to determine the total chloride content in solid samples [52, 53]. In this measurement, the surface of the sample is evaporated in a plasma with a high-energy laser. The plasma emits characteristic near-infrared radiation which can be detected and quantified. A limit of detection of 0.1–0.15 wt%, and a resolution of 2 mm is reported, as well as a good correlation with the acid-soluble method similar to µXRF [52, 54].

In addition to the direct measure on solid, a main advantage of µXRF or LIBS is that they also measure the concentration of other elements simultaneously. As such, further correlation with other elements is possible, such as magnesium phases precipitation during seawater exposure [55].

## 2.3 Equilibrium methods for measuring binding capacity

2.3.1 General description of the methods

The equilibrium method is a simple experimental concept to measure the binding isotherm. It involves immersing cementitious paste or mortar samples in an external chloride solution to attain equilibrium with the pore solution. The free chloride concentration in the pore solution is then considered equal to that of the external solution.

Zibara [56] has documented three distinct, chronological versions of the equilibrium method. In the first method, as used and documented by Blunk et al. [57], Byfors [58] and Tritthard [4], the bulk samples are simply immersed in a known chloride solution and the eventual decrease in its chloride concentration is determined upon achieving an equilibrium. The total chloride is determined by the difference in concentration between the initial and the equilibrium solution. However, this method can require up to 1 year of experimental time to reach equilibrium, as reported by Tritthard [4].

Alternatively, Sandberg and Larsson [59] used a second method where the chloride concentration was kept constant until equilibrium was reached. The total chloride can then be measured directly by acid-soluble chloride titration, and the bound chloride calculated if the porosity is known.

The third and the currently used version of the equilibrium method, developed by Tang and Nilsson [60], provides a much quicker evaluation of the bound chlorides. This technique involves exposing a ground cement paste sample to a chloride solution of known concentration and measuring the depletion after allowing sufficient time to achieve equilibrium. According to Tang and Nilsson, when a paste is wet-crushed and water-sieved to particle size of 0.25–2 mm, the adsorption equilibrium could be reached within 14 days, as shown in Fig. 3. The method uses 25 g of crushed sample dried at 11% RH, and immersed in a NaCl solution saturated with $Ca(OH)_2$. The chloride concentration is determined by potentiometric titration. The content of the bound chlorides is calculated by the following equation:
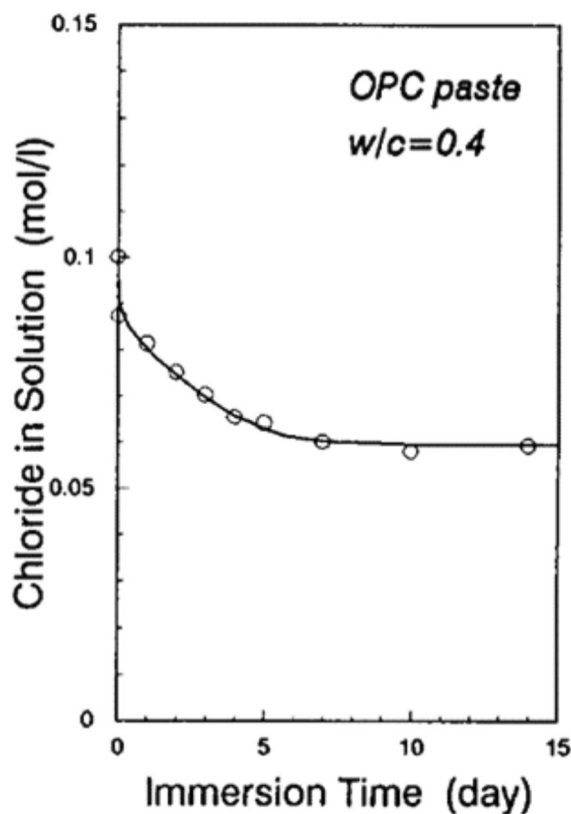
Fig. 3 Immersion time required to reach equilibrium between crushed cement paste and a NaCl solution (Reproduced with permission from [60])

$$C_b = \frac{M_{Cl}V(C_0 - C_1)}{W} \qquad (1)$$

where C_b is the bound chloride content (mg/g-sample); V is the volume of exposure solution (ml); C_0, and C_1 are the initial concentration and the equilibrium concentration of the exposure chloride solution (mol/l); and W is the weight of dry sample (g) that can be obtained from the difference in weight of the wet sample and the amount of free water. In the original publication, the amount of free water was estimated from the difference in weight of the sample dried in a desiccator at 11% RH and in an oven at 105°C [60]. In more recent work, the free water content has also been determined by drying at 40°C until constant mass by thermogravimetric analysis (TGA) [61] as ettringite and C–S–H can already lose bound water below 105°C [62].

The Tang and Nilsson method is the most used method today. It has been instrumental in assessing other chloride binding methods and it is therefore considered to be fairly accurate, as used and validated by several researchers [4, 9, 10, 63–65]. For example, Dhir et al.[63] used this equilibrium method to establish the chloride binding capacity of GGBS pastes compared to PC control pastes. Delagrave et al.[65] used the same method to evaluate the interaction mechanisms of chloride with hydration products of cement pastes with different concentrations of silica fume and clinker. Zibara [56] established a comprehensive discussion on the reproducibility of the Tang and Nilsson test procedure. De Weerdt et al. used the same method to study the chloride binding isotherms for well hydrated cement pastes exposed to $MgCl_2$, $CaCl_2$ and NaCl solutions of varying chloride concentrations [9]. The use of the equilibrium method to carry out a series of studies on the chloride binding capacity confirms the applicability of this method to varying cementitious systems including supplementary cementitious materials [10, 12, 13, 27].

2.3.2 Equilibration time for powdered samples versus paste discs

In general, the time taken for a sample to reach equilibrium has been observed to differ with respect to the sample size. Crushed particles have consistently shown significantly higher chloride binding rates than discs (or slices) [60, 66], i.e., discs generally take longer times to reach equilibrium. For instance, Arya et al. observed that discs of 6 mm thickness did not reach equilibrium after 84 days of immersion in 2% chloride solution [6]. Nevertheless, thinner discs (e.g., 1–3 mm) equilibrates faster and this shape of sample allows for further experiments [13], such as XRD on wet discs (see Sect. 3.2).

On the other hand, a few studies have observed crushed or powdered samples to demonstrate higher binding capacities than discs, leading to an overestimation of bound chlorides (or an underestimation by the disc method) [56, 67]. Smaller particle sizes of samples would also enable higher chances of carbonation and/or continuation of hydration [64, 68] in particular when wet-crushing and water sieving are used. The best choice of sample geometry is currently

Table 1 Sample and solution used in equilibrium chloride binding experiments

Sample type	Size or thickness	Sample mass (g)	Solution volume (mL)	Author, Date	References
Disc	1 cm			Tritthard (1989)	[70]
Crushed pieces	0.25–2 mm	25		Tang and Nilson (1993)	[60]
Crushed pieces	0.25–2 mm	25	30	Dhir et al. (1996)	[63]
Crushed pieces	0.25–2 mm	8	10	Jensen (2000)	[7]
Disc	3 mm	25	~100	Zibara (2001)	[27, 56]
Crushed pieces	0.2–2.5 mm	75		Baroghel et al. (2012)	[8]
Crushed pieces	<1 mm	30	15	De Weerdt et al. (2015)	[9]
Crushed pieces	5 mm	25	100	Sui et al. (2019)	[11]
Disc	2 mm	7	40	Wilson et al. (2022)	[13]
Crushed pieces	<2 mm	20	20	Baba Ahmadi et al. (2022)	[12]

unclear and should be decided based on the lab expertise, comparison to previous experiments, and/or requirements of associated experiments.

2.3.3 Mass of sample versus mass of solution

Table 1 summarizes the sample type, mass of sample and the volume of solution used in selected chloride binding experiments. The first observation is that the necessary information is not always provided by the authors, especially in older studies. This limits the potential comparison between these studies. This ratio between the mass of the sample vs. the volume of the solution changes the difference between initial concentration and the final concentration, as well as the buffering of the solution by the sample (e.g. pH, sulfate, …) or the potential carbonation. It is yet unclear which conditions should be preferred. For future analysis and modeling of these experiments, the necessary complementary data (pH, free chloride concentration, carbonation degree, …) should be provided by the authors [3, 69].

2.3.4 Type of exposure solution

The solutions are generally pure chloride solutions with specific associated cations such as sodium, calcium, or magnesium. Traditionally, sodium chloride solution seems to have been a major chloride solution of interest, however calcium and magnesium chloride solutions have also been a point of investigation as reported by [9, 70]. The effects of pH on chloride binding or leaching of calcium have also been investigated with NaOH and HCl solutions [4, 13, 61]. Moreover, attempts towards mimicking the pore solution of cementitious matrices have motivated the addition of $Ca(OH)_2$ and/or NaOH in chloride solutions [9, 13, 71]. Whether this method for simulation of pore solution is a preferred method or not, especially in systems with SCMs and varying pore solution characteristics is certainly a point of discussions. However, it is clear that the state of the solution needs to be considered for a generic approach to thermodynamic models [3].

Tritthard reported that prior to chloride exposure, slabs were soaked in a chloride-free solution to saturate capillary pores with water [4]. Three solutions were then employed: saturated $Ca(OH)_2$ (pH 12.5),

0.1 M NaOH (pH 13.0), and 0.5 M NaOH (pH 13.7), each with several chloride concentrations and associated cations. Tang and Nilsson utilized several concentrations of NaCl each saturated with $Ca(OH)_2$ [60]. Zibara used varying concentrations of NaCl [56]. De Weerdt et al. used varying concentrations of NaCl, $CaCl_2$ and $MgCl_2$ [9]. Hemstad et al. reported using varying concentrations of $CaCl_2$, NaCl and HCl [61]. Wilson et al. also compared the effect of buffering the pH of the equilibrium solution with 0.3 M NaOH (pH 13.0) or not (pH ~ 12.5) [13].

In general, a strong dependence on the pH of the exposure solution is observed, as expected by the strong dependence of physical and chemical binding on the pH [3, 19, 72]. Therefore, the choice of the exposure should be made with great care as a function of the goals of the study, and a sufficient amount of data needs to be reported for inter-study comparison.

2.4 Dissolution-based methods to measure binding capacity

These methods aim to extract chloride from the cementitious materials using an acid/water solution. The acidity of the solution and the harshness of the treatment (e.g., boiling the sample) dictate which classes of chloride are extracted from the sample. The solution can then be analyzed using the methods described in Sect. 2.1 to estimate the content of extracted chloride and assign them to one of the chloride classes shown in Fig. 1.

2.4.1 Water-soluble chloride

The concentration of chloride in the pore solution (free chloride) is one of the main factors in the drop in electrochemical potential that can lead to rebar depassivation [73, 74]. Therefore, it is important to have good methods to measure directly the concentration of chloride in the pore solution [5]. It is possible in theory to extract the pore solution using expression methods [75–78], although this is not suitable for routine measurements, especially in old concrete and high-performance concrete which require many samples to obtain a sufficient volume of pore solution for analysis.

The water-soluble set of methods ([79] and references therein) aims to extract the chloride by equilibrium with a neutral aqueous solution, similar to a

desorption experiment. Some variants require to correct the pH or the redox potential for example with hydrogen peroxide [23]. To accelerate the kinetics of desorption and transport out of the sample, the sample is crushed and the solution with the sample is heated [79]. The solution is allowed to rest for a given amount of time and, in some cases, reheated before being filtered. The solution can then be analyzed to measure chloride concentration, which has been interpreted as the free chloride content in the sample [79, 80]. This method was found to produce results similar to the pore solution expression methods [80].

The heating temperature and composition of the equilibrium solution are important for the reliability of the method [79, 80], to avoid extracting bound chloride, and/or the chloride in chloride containing aggregates rather than just the free chloride [81]. However, with a carefully designed method, it was shown that the desired reproducibility and repeatability can be obtained [79, 82]. This method is part of the ASTM C1218 standard [23].

This method was used as early as 1971 by Ramachandran [83] to investigate the interaction of chloride with C–S–H. The same method in combination with others advanced methods such as SEM–EDS was used 50 years later by Georget et al. to refine this investigation [20]. In particular, it was shown that some of the chloride absorbed on C–S–H is not accounted for by the water-soluble method, and therefore, this "irreversible fraction" should not be considered as participating in the mobile chloride fraction [3, 20]. Trejo and coworkers also used this method in several studies to quantify the suitability of current standards, especially regarding admixed chloride [84, 85].

2.4.2 Acid-soluble chloride

Although water-soluble and acid-soluble chloride determination methods have been developed around the same time [6, 86], the acid-soluble method has been more widely employed because of to its use in chloride profile determination [87].

Both methods are very similar. However, to also measure the chemically bound chloride, a harsher acidic solution is used to dissolve the chloride-containing hydrate phases. Typically, a heated nitric acid solution is used. The method is well established and

validated [5, 33] and is part of several standards [22, 88].

The bound chloride content is often estimated by difference between the total and free chloride contents. This assumption was investigated in several studies [11, 13] and seems to be valid at a first glance, even if some variations are observed that could be attributed to the uncertainties of the many experiments required for such a verification.

It was shown by Trejo et al. [84] that defining thresholds on the acid or on the water-soluble chloride is not equivalent. In particular, the ratio between acid-soluble and water soluble is highly dependent on the binder. This was explained by Wilson et al. who demonstrated that the binding mechanisms can be very different between binders, due to the changes in phase assemblage, in particular the ratio of C–S–H and aluminum hydrates [13].

2.5 Fitting bulk diffusion profile to estimate chloride binding

Surface concentrations extrapolated from chloride profiles can be used to estimate chloride binding capacity. Using the acid-soluble method as a function of depth for in situ samples, it is possible to obtain profiles of total chloride content, commonly known as chloride profiles [3, 89], such as the one in Fig. 2. These profiles look like diffusion profiles, as such they have been modeled with Fick's second law, as is shown in Eq. (2):

$$\frac{\partial C}{\partial t} = D_{app} \frac{\partial^2 C}{\partial x^2} \tag{2}$$

where $C(x, t)$ is the total chloride concentration, D_{app} is the apparent chloride diffusion coefficient, t is the exposure time, and x is the distance from the exposed concrete surface. It is important to note that $C(x, t)$ is a total chloride content, also including "immobile chloride". As such, D_{app} is called apparent because it also includes information about the binding. Such an approximation is only valid under the assumption of a linear binding isotherm [89, 90].

Assuming one-dimensional diffusion in a semi-infinite medium, Fick's second law can be solved analytically assuming that the surface chloride concentration C_s remains constants, i.e. [91]:

$$C(x = 0, t > 0) = C_s. \tag{3}$$

The analytical solution for Fick's second law for this case is given by:

$$C(x, t) = C_0 + (C_s - C_0)\,\mathrm{erfc}\left(\frac{x}{2\sqrt{D_{app}t}}\right) \tag{4}$$

where C_0 is the initial chloride concentration of concrete before exposure to the chloride environment.

Using Eq. 4, the surface concentration can be extrapolated from a chloride profile as shown in Fig. 4. However, a major argument against the use of this method is that the analysis of real chloride profiles clearly indicates that the chloride profile is not constant with time, and a peaking/plateauing behavior is often observed in profiles due to phenomena such as leaching [3, 61, 69]. Thus, the Cs value is a fitting parameter rather than the actual maximum binding for a given exposure solution (which is limited by the binding capacity at a given pH and therefore closer to the value at the peak of the profile). Although some empirical corrections can be added to make the surface concentration dependent on time, it breaks the fundamental assumption of the Fick's law analysis of these profiles [89, 90]. Another method is to not fit the first few points, which can add a bias from the user. The method was used extensively by Zibara [56, 92] and compared to the equilibrium method. The same order of magnitude was found but slightly higher values were obtained with the bulk diffusion method. As such, the equilibrium method is typically preferred in current lab studies of chloride binding.
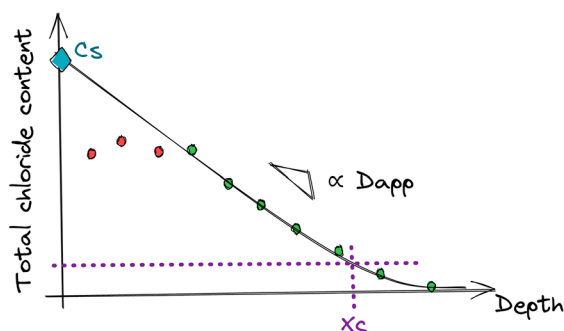
Fig. 4 Determination of the chloride binding capacity by fitting a bulk diffusion profile (reproduced with permission from [3]). C_s does not necessarily represent the value of the first measurement point due to leaching effects

A possible unique use of the surface extrapolation method is the extraction of binding capacity from field samples.

3 Chloride quantification by phase

As highlighted in the previous section, the results of the bulk methods are useful to compare the overall binding capacity of binders. However, for fundamental investigations that can reveal mechanistic insights, it is necessary to rely on methods that characterize the individual contribution of each phase to the overall chloride binding.

3.1 Pure phase synthesis

A first method to analyze chloride binding of individual phase is to synthesize homogeneous pure phases or model systems and measure the chloride binding capacity using the methods detailed in the previous sections [15, 20, 72, 93–95]. The information can then be extrapolated to the conditions in hardened cement pastes to interpret their overall binding capacity. A main challenge is to ensure that representative phase are synthetized, whether for C–S–H (e.g. representative Ca/Si, Al/Si) [96] or for AFm phases [16].

3.2 XRD

The elastic scattering of X-ray by crystalline materials creates characteristic diffraction patterns due to the constructive interferences, determined by the lattice structure of these materials. The comparison of experimental diffractograms to experimental or theoretical diffractograms of pure phases allows to identify, and quantify the crystalline phases, as well as infer their lattice structure [97]. X-ray diffraction (XRD) has been increasingly used in cement science in the last decades due to the general availability of the method in materials characterization laboratories and its usefulness in quantifying the phase assemblage of cementitious materials [97]. With regard to chloride binding, XRD allows for the identification and the quantification of chemical binding in the AFm family of phases. The main Cl-bearing AFm phases are Friedel's salt (Fs, $X = Cl^-$, an end-member of the hydrocalumite) and Kuzel's salt ($X = 0.5\ Cl^-$, $0.5\ SO_4^{2-}$).

The main diffraction peak of Fs (002) occurs at ~ 11.35° 2θ (CuKα radiation source). XRD has been used for the identification and semi-quantitative estimation of Fs content with the intensity/area of this peak in different types of binders and conditions, for example, to investigate: blended-cement systems with slags, fly ash and pozzolans [98, 99], the carbonation of Fs in concrete [100], the occurrence of Fe-containing Fs in hydrated synthetic aluminoferrite pastes [101], the carbonation of Fs in calcium aluminate cement systems [102], the semi-quantitative comparison of Fs originating from pozzolan and Portland cement [103] and their synergetic effects [104], the uptake of chloride and carbonate by Mg–Al and Ca-Al layered double hydroxides in simulated pore solutions of alkali-activated slag cement [105], the chloride binding in mortars with alumina-rich cementitious materials and seawater [106], in Portland composite cements containing metakaolin and silica fume [12], and more. This type of analysis can be complemented by quantitative measurement of Fs, for example in sulfoaluminate cements (compared to ^{27}Al MAS NMR measurements) [107] or in hydrated Portland cement–metakaolin–limestone blends (compared to thermodynamic modelling) [108].

Structural investigations showed a phase transition of Fs at about 30°C from a monoclinic to a rhombohedral phase, also known as, resp., low temperature and high temperature polymorphs of Fs [72, 109, 110].

Although the high temperature polymorph is the most common and often the only polymorph observed in cement and concrete applications. Further investigations showed the interchangeability of anions in the AFm structures, e.g., chloride can displace hydroxide, sulfate and carbonate [15]. As shown in Fig. 5a, different solution compositions lead either to Friedel's salt solid solutions or combinations of pure phases [15]. Further investigations on hydrated cement pastes and synthetized AFm phases showed a wide range of solid solutions [16] with chloride, carbonates, sulfates and hydroxyl ions. Figure 5b shows the gradual shift of the interlayer peak from high temperature rhombohedral phase hemicarbonate (10.76°2θ) to high temperature rhombohedral Friedel's salt (11.35°2θ), with increasing chloride/carbonate ratios (χ_{2Cl}=2Cl/Ca) [16].

With a better understanding of Fs and its solid solutions (Fs_{ss}), it then becomes possible to quantify the chemically bound chloride in AFm with quantitative Rietveld analyses from the measurement of the stoichiometry of the Fs_{ss}. Experimental protocol for XRD diffraction on hydrated cement pastes has been optimized over the years, as described in [97]. An important consideration is the analysis of fresh slices instead of dried powders, as hydrates may decompose or transform during solvent exchange and drying, leading for example to lower ettringite contents [97] or jumps in solid-solution series as in Fig. 5b [16].
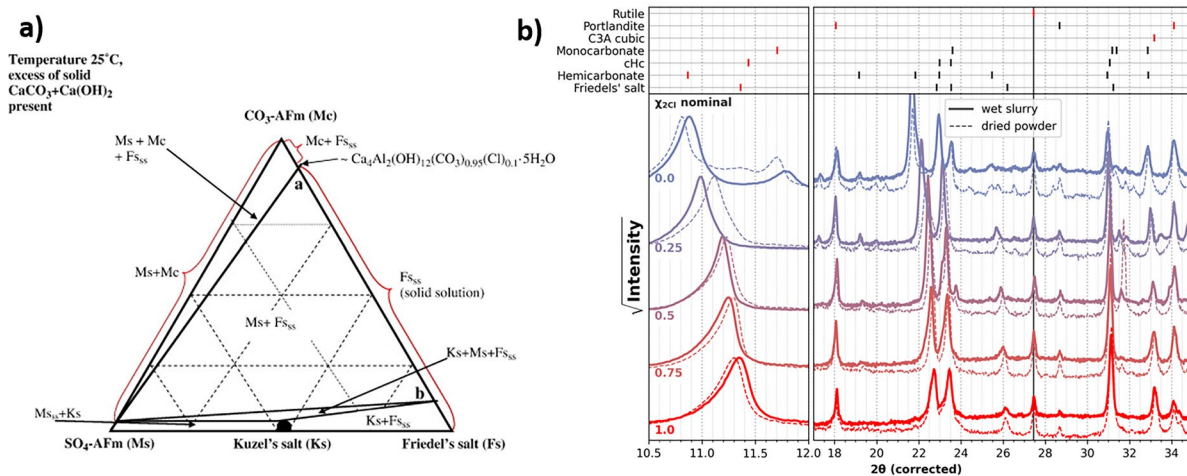
Fig. 5 **a** Schematic phase relations at 25°C, between Friedel's salt, monosulfoaluminate and monocarboaluminate (reproduced with permission from [15]). **b** Powder XRD diffracto-grams for the wet and dried samples in the chloride series, in which only high temperature polymorphs are observed (reproduced with permission from [16])
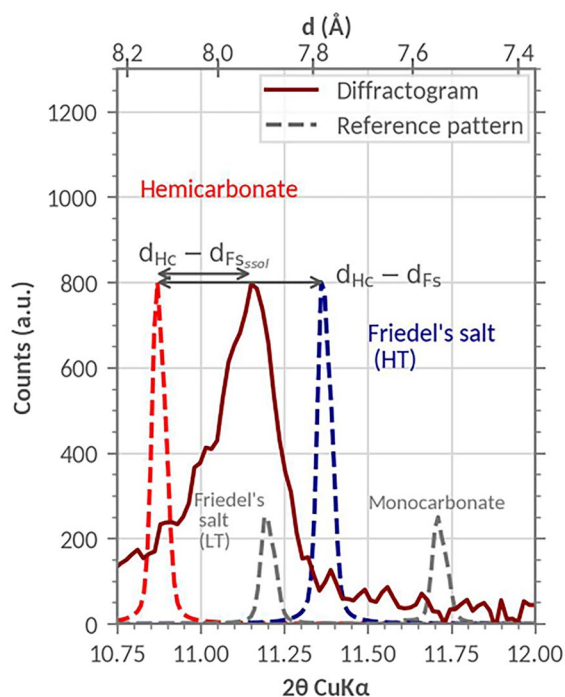
Fig. 6 Using the 002 peak of XRD patterns to estimate the stochiometric ratio (χ_{2Cl}) of Friedel's salt solid solutions (reproduced with permission from [13])

The external standard method [111] has been successfully used to quantify crystalline phase contents in hydrated cement pastes containing amorphous phases (e.g., C–S–H). More specifically, both the stoichiometry and the content of the Fs_{ss} can be obtained from XRD patterns, as proposed in [11, 13, 16, 112]. The χ_{2Cl} proportion of chloride and carbonate in Fs_{ss} can be determined from the d-spacing of the 002 peak as shown in Fig. 6, with $\chi_{2Cl} = (d_{Hc} - d_{Fsss})/(d_{Hc} - d_{Fs})$ [13]. This approach was validated for different series of systems with SEM–EDS hypermap chemical analyses [11, 13, 16] (see Sect. 3.4). The chemically bound chloride content can then be calculated with both χ_{2Cl} and the mass fraction of Fs_{ss} obtained with a Rietveld analysis with the external standard (an HighScore Plus template of anhydrous phases and hydrates for such analysis can be found in the supplementary materials of [13]).

Using XRD to characterize chemical chloride binding has the important advantage of allowing with a single analysis the quantification of both the stoichiometry and the mass fraction of Friedel's salt. XRD scans on the same samples are highly reproducible

and can generally provide repeatable results with different samples of the same material in the same exposure conditions [113]. However, the Rietveld refinement method for complex materials (e.g., hydrated cement pastes) with several phases and overlapping peaks is challenging and requires user choices which can vary between the analysts. Although general guidelines exist for the refinement of hydrated cement pastes [97], the results should not be overinterpreted as their quality may be impacted by the analyst experience. Furthermore, the analysis of new or alternative systems can generate new challenges. For example, when quantifying Fs in systems with higher Mg content (e.g., systems with ground granulated blast furnace slags), one needs to be careful with the overlap of the hydrotalcite peak, which can eventually be distinguished with higher resolution scans [17].

3.3 TGA

Thermogravimetric analysis (TGA) is a technique in which the mass of a sample is monitored while it is exposed to a controlled temperature regime. Commonly, for cementitious materials, the specimen is a finely ground powder, of around 40 mg in most equipment, that is heated from room temperature to high temperature (~ 1000 °C) in a nitrogen atmosphere. Hydration stoppage may be employed, although it is not always done. The weight loss is associated with loss of volatile components such as water (40–600 °C), or CO_2 (550–1000 °C). The weight loss of each cement paste phase occurs at tabulated temperature ranges [62, 114–117]. These ranges are approximate, and exact values depend on heating rate, phase amounts, powder fineness, among other factors [62, 118]. When the stoichiometry is known/fixed, the mass loss can be used to calculate phase amounts. Arguably, the most common use of TGA in cement science is to quantify contents of calcium hydroxide, calcium carbonate, and bound water.

TGA can also be used to quantify Friedel's salt, which has two peaks of water loss (dehydroxylation), as shown in Fig. 7. The first is from 100 to 150 °C and is often not identifiable due to peak overlap. The second, from 230 to 410 °C, is associated with the loss of six main layer water molecules associated to the chloride site in Friedel's salt. This peak is typically used to quantify Friedel's salt, as discussed in [26], or in the case of Friedel's salt solid solution, the

Fig. 7 Determination of chloride in Friedel's salt using thermogravimetric analysis (reproduced with permission from [26])
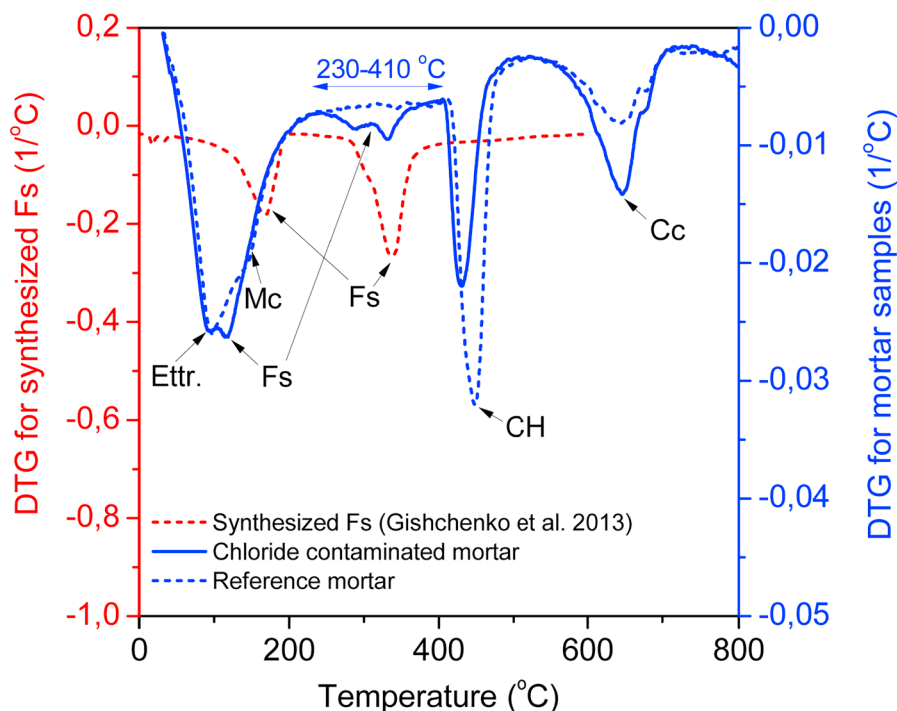

chloride content in Fs_{ss} [13, 16]. The peak has some overlap with calcium hydroxide and hydrotalcite but, without peak overlap, it is an easy and rapid way to quantify Friedel's salt amount.

Using TGA, complemented by other techniques, it has been shown that the amount of Friedel's salt increases: with increasing NaCl concentration; when Al sources such as fly ash or metakaolin are used to replace cement; and when $CaCl_2$ is used for binding instead of NaCl [108, 119].When cement pastes are exposed to high concentrations of $CaCl_2$ at relatively low temperatures (below 23 °C), the calcium hydroxide reacts to form calcium oxychloride. While most chloride binding studies are not carried out in such conditions, the formation of calcium oxychloride is a major contributor to chloride binding in these conditions. The amount of calcium hydroxide, determined from TGA, can be used to predict the amount of calcium oxychloride that forms rather precisely based on stoichiometry [18, 120]. Pure calcium oxychloride phases also show characteristic TGA responses with multiple peaks, for example, for $3Ca(OH)_2 \cdot CaCl_2 \cdot 12H_2O$, at 83 °C, 400 °C, and 540 °C [121]. Although a different TGA response can be obtained in real samples as these phases are often dried or carbonated.

3.4 SEM

The electron beam of a scanning electron microscope (SEM) interacts with the sample in many different ways. One of them is the production of characteristic X-ray, which can be detected and identified by energy dispersive spectroscopy (EDS). EDS allows to measure the spatial concentration of elements and relate them to other information from the SEM, including microstructure features, e.g. observed from backscatter electrons (BSE) [122]. Due to its measurement principle, SEM–EDS is not able to measure hydrogen [123], and lighter elements (e.g., oxygen, sodium) have increased uncertainties [124]. The spatially resolved information allows investigations as a function of distance, e.g., the depth from an exposed surface [55, 69, 125]. The spectra can be used to identify elements and quantify concentrations, using a semi-quantitative approach for simplicity or quantitatively after calibration with standards. Plotting the atomic % of selected elements as ratios allows different phases to be distinguished (e.g., different AFm phases) and also changes in composition to be determined (e.g., Ca/Si ratio of C–S–H) [122, 125, 126]. In addition, this process also facilitates interpreting the results, as the interaction volume of the electron beam with
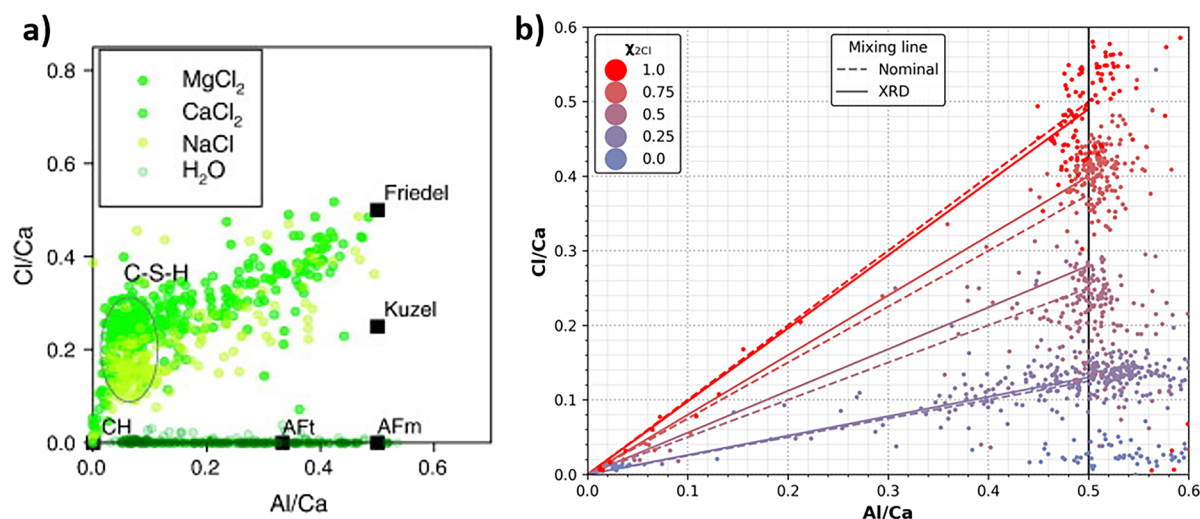
Fig. 8 AFm phases detection by SEM–EDS in systems **a** without (reproduced with permission from [9]) or b with (reproduced with permission from [16]) limestone

the sample means that mixture of phases are detected [122, 125–127]. The use of ratio plots to analyze the chloride content in C–S–H and AFm phases is demonstrated in Fig. 8.

Samples for SEM–EDS analysis are normally hydrated and chloride-exposed cementitious materials (paste, mortar or concrete). The samples can be in the form of cut/sawn slices or crushed pieces of well-hydrated cement pastes. Sample preparation for SEM–EDS is crucial for a good analysis as a flat surface is required [122, 128]. Drying of the sample is also required, and to preserve the microstructure, solvent exchange is preferred [122, 129]. The drying step should not interfere with the chloride distribution in the samples. Machner et al. [10] showed that common solvent exchange procedures might not be sufficient to replace all chloride-containing pore solution if the samples have been exposed to solutions of high chloride concentrations (e.g. ≥ 2 mol/L) and can result in chloride salt (e.g. NaCl) precipitation in the dried samples after solvent exchange. Alternatively, one can wash the samples carefully with a limited volume of deionized water prior to common solvent exchange procedures in order to remove all chloride from the pore solution. This has been investigated by Plusquellec et al. [130] in order to study the alkali content in the pore solution of hardened and ground concrete samples. However, it was shown that alkali chloride salt precipitation cannot fully explain the

chloride concentration in solid phases observed in hydrated C_3S pastes after exposure at 0.5 mol/L [20].

SEM–EDS has been used by many authors to describe changes in the AFm, or C–(A–)S–H compositions upon chloride exposure. Beaudoin et al. provided an early analysis of Cl binding on C–S–H and proposed two types of binding [95], which was later confirmed by Georget et al. [20]. De Weerdt et al. [131] used dot plots from SEM–EDS point analysis to describe the effect of magnesium and sulfur in sea water on the chloride binding of well-hydrated cement pastes. In addition, they showed the impact of the associated cation (Na^+, Ca^{2+}, or Mg^{2+}) [9] and the effect of sea water [132] during chloride exposure on the chloride content in AFm and C–S–H. The effect of sea water compared to NaCl on chloride ingress and chloride binding was also investigated in concrete samples by SEM–EDS [133]. Based on these observations, Hemstad et al. [61] used SEM–EDS dot plots to investigate the change in the Cl/Al ratio of Cl-AFm (Fs_{ss}) in well-hydrated cement pastes exposed to chloride at different pH. Similarly, Machner et al. [10] showed the impact of pH and calcium activity on the chloride content in hydrotalcite formed in cement pastes containing dolomite and no or small amounts of metakaolin. These analyses can also be carried out on SEM–EDS hypermaps which, for example, can be used to estimate the chloride speciation across the

ingress front to investigate the in-situ binding isotherm, with detailed speciation [125].

The effect of pH on the chloride content in AFm phases could also be shown with SEM–EDS by [69] in mortar samples that were exposed to unidirectional chloride diffusion at different pH. The Cl/Al ratio (for AFm) or Cl/Si ratio (for C–S–H) was determined by point analyses not just as a bulk analysis of the cement matrix, but obtained in a spatially defined area to allow the evaluation of the data as a function of the depth from the exposed surface [69]. This concept was based on the evaluation by De Weerdt et al. [134], who showed a depth-dependent chloride content of C–S–H in long-term marine exposed concrete. In addition, SEM–EDS was used to determine the impact of various binders on long-term chloride profiles of concrete [135]. Wilson et al. used it to investigate the distribution of bound chloride between AFm and C–S–H in Portland limestone cement pastes and blended systems [11, 13, 20].

3.5 NMR

Nuclear magnetic resonance relies on the measurement of the resonance of magnetic nuclei spin in a magnetic field. Both static (chemical displacements) and dynamic (characteristic relaxation times) properties can be measured. Chlorine has two stable isotopes ^{35}Cl (~75% abundance) and ^{37}Cl (~25% abundance). They are both NMR active but both isotopes are quadrupolar nuclei (spin 3/2) with very broad peaks. Thus, Cl NMR is challenging and ^{35}Cl is generally preferred for its abundance [136].

As such, there are only a few studies that have used ^{35}Cl NMR for cementitious materials. Kirkpatrick et al. [137] utilized ^{35}Cl NMR to investigate AFm phases (layer double hydroxides of the hydrocalumite family). In particular, Friedel's salt's phase change between the low and the high temperature polymorph at 6°C was observed. NMR is sufficiently sensitive to measure the impact of relative humidity. As for other AFm phases [138], structural changes can be observed linked to the loss of water in the crystal interlayer. The Friedel's salt signature was also used by Barberon et al. to investigate the impact of chloride on hydration by solid NMR [139]. Yu and Kirkpatrick [140] analyzed the ^{35}Cl relaxation in hydrate suspensions. However, it is not clear what is measured exactly as the largest chloride binding capacity

has been found for the portlandite, which is nowadays neglected in most models, and further improvement to the method is required. Cano et al. [141] studied chloride penetration caused by capillary absorption advection in low- and high-permeability mortars. The authors could demonstrate that chemical and physical bound chloride were detected. Free chloride was also detected by Yun et al. using NMR in damaged sidewalk concrete exposed for 20 years to the environment [142]. Ji et al. further refined the relaxation study using an imaging equipment [143] which could in theory be used to study chloride ingress. By focusing on $^{35}Cl^-$, $^{23}Na^+$ and $^{1}H^+$ NMR may provide such information, non-destructively and continuously with a dedicated imaging equipment developed by Pel and coworkers [144]. It has been applied to the early hydration of cementitious materials, in particular to investigate the ratio of bound chloride to bound sodium. This equipment was further used to follow chloride ingress. However, due to the difficulty to measure Chloride, the ^{23}Na signal was used. As sodium and chloride diffusion are not necessarily linked during chloride ingress the application of this technique needs to be carefully interpreted [3].

Similarly, Friedel's salt formation can also be studied by ^{27}Al solid state NMR [7, 12, 145, 146]. However, due to the special equipment and the expert knowledge required, the advantages of this method are still unclear compared to, for example, XRD or TGA. Therefore, the application of solid NMR to chloride content determination seems limited currently. However, solid state NMR as a key role to play in the complementary characterization of the phase assemblage to better understand the impact of the SCM mineralogy on chloride binding [12].

3.6 Thermodynamic modelling

Thermodynamics is an essential instrument for characterizing equilibrium phase assemblages in cementitious systems and it has been effectively utilized in various areas of cement research, such as studying cement hydration [21, 147, 148] and durability [9, 108, 149]. Geochemical modeling applications like GEMS [150] or PHREEQC [151] allow the computation of the equilibrium phase assemblages as a function of composition, temperature, and pressure. However, the effectiveness of thermodynamic calculations is contingent upon the availability of a detailed

database containing the thermodynamic properties of cement-based materials [21, 152, 153].

Unlike simpler empirical chemical models, thermodynamic models aim to provide a full coupling between the solid phases and the solution at equilibrium with these phases. As such, it can be used to easily investigate the impact of pH, NaCl concentration or even the co-cations on the chloride binding. Of course, this assumes that the database of thermodynamic properties is sufficiently accurate to model such effects. Due to the current limitations of the software and databases, the application of thermodynamic modeling in chloride binding studies is divided into three aspects: (1) the determination of the initial hydrated phase assemblage to interpret other binding experiments such as the estimation of C–A–)S–H content [13], (2) the determination of the phase assemblage, including the Friedel's salt content (chemical binding), and (3) the sorption of chloride on solid surfaces (physical binding, mostly on C–(A–)S–H). Modelling both chemical and physical binding requires an iterative process in most software [154], although it is theoretically possible in GEMS [150].

For the study of chemical binding with thermodynamic modelling, two cases must be distinguished based on the AFm phases present. Without limestone, or other carbonates available in the cement, the dominant AFm is the monosulfate. In this now rare case in modern cement, thermodynamic modelling has shown to provide reliable predictions for chloride binding, including the prediction of Kuzel's salt [15, 155, 156]. It allows to investigate the influence of the chloride salt [9] or the impact of SCMs [108] in limestone-free systems.

When limestone is present, the stable AFm phases are hemicarbonate and monocarbonate [16, 72, 157]. In this case, a ternary solid solution is observed between hemicarbonate and Friedel's salt (HO^-–Cl^-–CO_3^{2-}–AFm) [16, 72, 158]. This solid solution is poorly investigated, and no solid solution model fully explains all the available experimental data, in particular the correct end-members to consider are not well-defined [16]. As such the chloride binding of limestone-containing system cannot yet be adequately predicted by thermodynamic modelling. This is a clear limitation of thermodynamic models for modern cementitious binders. Similarly, calcium oxychloride compounds are also not present in common databases.

The use of thermodynamic models, in particular sorption models can also be useful to study physical binding. The pioneering work of Elakneswaran and co-authors [19, 159, 160] has proposed a surface complexation model to describe chloride binding on C–(A–S–H surfaces. The complexation model was calibrated using zeta potential measurements and validated with chloride binding measurements for OPC and cement blended with slags. However, the extrapolation of this model to other systems is uncertain due to the lack of a validated thermodynamic model for C–A–S–H. In particular, the effective Ca/Si, Al/Si and S/Si ratios still need to be measured for accurate thermodynamic simulations.

Even with these limitations, thermodynamic modelling is one of the only tools which allows the extrapolation of real-life chloride ingress from the controlled chloride binding lab experiments [3]. A good example is the work by De Weerdt et al. [132, 133] comparing ingress in NaCl solution and in seawater, or the analysis of the impact of leaching [61, 69]. Although semi-quantitative mechanisms can be uncovered, a truly quantitative description is only possible if limitations described previously are solved.

4 Conclusion

In this review, the different methods to measure the chloride speciation in cementitious materials were presented. They are summarized in Table 2. First, the bulk methods to measure the total chloride, and the chloride binding isotherm (free chloride, and bound chloride) were described. The wet chemistry methods (acid-soluble, wet soluble) are well established but their interpretation in terms of chloride speciation (chemical or physical binding) is not straightforward. New measurements methods on solids have been introduced (μXRF, LIBS) to simplify the measurements. These methods have a reasonable agreement with wet chemistry methods. Several studies have shown that the chloride binding measurement should take place in conditions that are well controlled (pH, cations, extra anions, sample size). In particular, the use of chloride profiles to determine the binding capacity is not recommended due to leaching effects.

Table 2 Summary of the methods investigated in this review

Method	Observation	Limitations
Water-soluble chloride	Free chloride content	Are all free Cl, mobile Cl?
Acid-soluble chloride	Total chloride content	No information on Cl speciation
μXRF/LIBS	Total chloride content	No information on Cl speciation Limited availability of the equipment
XRD	Chemical-bound chlorides in crystalline phases (AFm)	Sample preparation critical Limited availability of the equipment and expertise No information on physisorption
TGA	Chemical-bound chlorides in selected phases (AFm, hydrotalcite)	No information on physisorption
SEM–EDS	Stoichiometries of Cl-containing solid solutions (AFm) Stoichiometries of Cl adsorbing phases (C–S–H)	Only stoichiometries can be inferred, not content Limited availability of the equipment, sample preparation
NMR	Chemical and Physical bound chloride detection, and quantification per phases	Limited availability of the equipment and expertise Low sensitivity

More advanced methods have been developed to analyze the chloride binding by phase (e.g., AFm, C–A–S–H) such as XRD, TGA and SEM–EDS. These methods require higher expertise but they have the potential to provide quantitative information about the binding capacity of individual phases, in addition to other chemical information about the specimens. In terms of chemical binding, different methods are available to measure the binding capacity of each phase, with analyses generally focusing on the AFm phases. The most widely applicable methods are XRD and TGA. The physical binding is much harder to quantify accurately, and currently only a combination of phase assemblage estimation (using mass balance or thermodynamic approaches) and SEM–EDS analysis provides a satisfactory answer.

When the bulk and the by-phase methods are combined, it can be shown that the agreement is adequate in simplified systems, for OPC or blended systems. However, the issue of chloride classification remains open. Whether a chloride species is bound, free, water or acid soluble is crucial for the interpretation of experiments, and relating phase assemblage to durability performance. The division into mobile and immobile chloride is also a requirement for chloride ingress modelling. The main challenge is the lack of generic mechanistic models to predict the binding capacity of each phase individually to interpret experiments with confidence.

Another challenge identified by this review is the lack of report of secondary characterization experiments (e.g., pH of exposure solution, phase assemblage, degree of hydration, degree of carbonation, …) that are required to compare with confidence experiments carried out in different laboratories. The future work of this committee will be to propose recommendations on: (1) the choice of methods depending on the specific scientific objectives and (2) the secondary characterization experiments to report alongside the results of these methods to future-proof new chloride binding studies.

Data availability   No new data were created during the preparation of this manuscript.

Declarations

Competing interests   The authors declare that they have no competing interests.

References

1. Angst UM (2018) Challenges and opportunities in corrosion of steel in concrete. Mater Struct 51:4. https://doi.org/10.1617/s11527-017-1131-6

2. Angst UM, Geiker MR, Alonso MC, Polder R, Isgor OB, Elsener B, Wong H, Michel A, Hornbostel K, Gehlen C, François R, Sanchez M, Criado M, Sørensen H, Hansson C, Pillai R, Mundra S, Gulikers J, Raupach M, Pacheco J, Sagüés A (2019) The effect of the steel–concrete interface on chloride-induced corrosion initiation in concrete: a critical review by RILEM TC 262-SCI. Mater Struct 52:88. https://doi.org/10.1617/s11527-019-1387-0

3. De Weerdt K, Wilson W, Machner A, Georget F (2023) Chloride profiles—What do they tell us and how should they be used? Cem Concr Res 173:107287. https://doi.org/10.1016/j.cemconres.2023.107287

4. Tritthart J (1989) Chloride binding in cement II. the influence of the hydroxide concentration in the pore solution of hardened cement paste on chloride binding. Cem Concr Res 19:683–691. https://doi.org/10.1016/0008-8846(89)90039-2

5. Dhir RK, Jones MR, Ahmed HEH (1990) Determination of total and soluble chlorides in concrete. Cem Concr Res 20:579–590. https://doi.org/10.1016/0008-8846(90)90100-C

6. Arya C, Buenfeld NR, Newman JB (1990) Factors influencing chloride-binding in concrete. Cem Concr Res 20:291–300. https://doi.org/10.1016/0008-8846(90)90083-A

7. Jensen OM, Korzen MSH, Jakobsen HJ, Skibsted J (2000) Influence of cement constitution and temperature on chloride binding in cement paste. Adv Cem Res 12:57–64. https://doi.org/10.1680/adcr.2000.12.2.57

8. Baroghel-Bouny V, Wang X, Thiery M, Saillio M, Barberon F (2012) Prediction of chloride binding isotherms of cementitious materials by analytical model or numerical inverse analysis. Cem Concr Res 42:1207–1224. https://doi.org/10.1016/j.cemconres.2012.05.008

9. De Weerdt K, Colombo A, Coppola L, Justnes H, Geiker MR (2015) Impact of the associated cation on chloride binding of Portland cement paste. Cem Concr Res 68:196–202. https://doi.org/10.1016/j.cemconres.2014.01.027

10. Machner A, Zajac M, Ben Haha M, Kjellsen KO, Geiker MR, De Weerdt K (2018) Chloride-binding capacity of hydrotalcite in cement pastes containing dolomite and metakaolin. Cem Concr Res 107:163–181. https://doi.org/10.1016/j.cemconres.2018.02.002

11. Sui S, Wilson W, Georget F, Maraghechi H, Kazemi-Kamyab H, Sun W, Scrivener K (2019) Quantification methods for chloride binding in Portland cement and limestone systems. Cem Concr Res 125:105864. https://doi.org/10.1016/j.cemconres.2019.105864

12. Babaahmadi A, Machner A, Kunther W, Figueira J, Hemstad P, De Weerdt K (2022) Chloride binding in Portland composite cements containing metakaolin and silica fume. Cem Concr Res 161:106924. https://doi.org/10.1016/j.cemconres.2022.106924

13. Wilson W, Gonthier JN, Georget F, Scrivener KL (2022) Insights on chemical and physical chloride binding in blended cement pastes. Cem Concr Res 156:106747. https://doi.org/10.1016/j.cemconres.2022.106747

14. De Weerdt K (2021) Chloride binding in concrete: recent investigations and recognised knowledge gaps: RILEM Robert L'Hermite medal paper 2021. Mater Struct 54:214. https://doi.org/10.1617/s11527-021-01793-9

15. Balonis M, Lothenbach B, Saout GL, Glasser FP (2010) Impact of chloride on the mineralogy of hydrated Portland cement systems. Cem Concr Res 40:1009–1022. https://doi.org/10.1016/j.cemconres.2010.03.002

16. Georget F, Lothenbach B, Wilson W, Zunino F, Scrivener KL (2022) Stability of hemicarbonate under cement paste-like conditions. Cem Concr Res 153:106692. https://doi.org/10.1016/j.cemconres.2021.106692

17. Khan MSH, Kayali O, Troitzsch U (2016) Chloride binding capacity of hydrotalcite and the competition with carbonates in ground granulated blast furnace slag concrete. Mater Struct 49:4609–4619. https://doi.org/10.1617/s11527-016-0810-z

18. Jones C, Ramanathan S, Suraneni P, Hale WM (2020) Calcium oxychloride: a critical review of the literature surrounding the formation, deterioration, testing procedures, and recommended mitigation techniques. Cem Concr Compos 113:103663. https://doi.org/10.1016/j.cemconcomp.2020.103663

19. Elakneswaran Y, Iwasa A, Nawa T, Sato T, Kurumisawa K (2010) Ion-cement hydrate interactions govern multi-ionic transport model for cementitious materials. Cem Concr Res 40:1756–1765. https://doi.org/10.1016/j.cemconres.2010.08.019

20. Georget F, Bénier C, Wilson W, Scrivener KL (2022) Chloride sorption by C-S-H quantified by SEM-EDX image analysis. Cem Concr Res 152:106656. https://doi.org/10.1016/j.cemconres.2021.106656

21. Scrivener KL, Matschei T, Georget F, Juilland P, Mohamed AK (2023) Advances in hydration and thermodynamics of cementitious systems. Cem Concr Res 174:107332. https://doi.org/10.1016/j.cemconres.2023.107332

22. ASTM C1152/C1152M-04(2012)e1 (2012) Standard test method for acid-soluble chloride in mortar and concrete. ASTM International, West Conshohocken

23. ASTM C1218/C1218M-17 (2017) Test method for water-soluble chloride in mortar and concrete. ASTM International

24. Yang Y, Patel RA, Churakov SV, Prasianakis NI, Kosakowski G, Wang M (2019) Multiscale modeling of ion diffusion in cement paste: electrical double layer effects. Cem Concr Compos 96:55–65. https://doi.org/10.1016/j.cemconcomp.2018.11.008

25. Ferjaoui K (2022) Nanoscale modelling of ionic transport in the porous C–S–H network. EPFL

26. Shi Z, Geiker MR, Lothenbach B, Weerdt KD, Garzón SF, Enemark-Rasmussen K, Skibsted J (2017) Friedel's salt profiles from thermogravimetric analysis and thermodynamic modelling of Portland cement-based mortars exposed to sodium chloride solution. Cem Concr Compos 78:73–83. https://doi.org/10.1016/j.cemconcomp.2017.01.002

27. Thomas MDA, Hooton RD, Scott A, Zibara H (2012) The effect of supplementary cementitious materials on chloride binding in hardened cement paste. Cem Concr Res 42:1–7. https://doi.org/10.1016/j.cemconres.2011.01.001

28. Khanzadeh Moradllo M, Sudbrink B, Hu Q, Aboustait M, Tabb B, Ley MT, Davis JM (2017) Using micro X-ray fluorescence to image chloride profiles in concrete. Cem Concr Res 92:128–141. https://doi.org/10.1016/j.cemconres.2016.11.014

29. The American Association of State Highway and Transportation Officials (2021) AASHTO T 260-21 standard method of test for sampling and testing for chloride ion in concrete and concrete raw materials. AASHTO

30. NT BUILD (1996) 208 Concrete, hardened: chloride content by volhard titration, Edition 3. NORDTEST

31. Tang L (1998) Measurement of chloride content in concrete with blended cement. An evaluation of repeatability and reproducibility of the commonly used test methods. Nordtest Project 1410-98

32. Potgieter SS, Potgieter JH, Panicheva S (2004) Investigation into methods of chloride analysis of South African cement and cement-related materials with low chloride concentrations. Mater Struct 37:155–160. https://doi.org/10.1007/BF02481614

33. Castellote M, Andrade C (2001) Round-robin test on chloride analysis in concrete—part I: analysis of total chloride content. Mater Struct 34:532–549. https://doi.org/10.1007/BF02482181

34. Small H (1989) Ion chromatography. Springer, Boston

35. Pohl C (2021) Chapter 3—Stationary phases in ion chromatography. In: Pohl C, Avdalovic N, Srinivasan K (eds) Separation science and technology. Academic Press, pp 43–156

36. Srinivasan K (2021) Chapter 4—Suppressors in ion chromatography. In: Pohl C, Avdalovic N, Srinivasan K (eds) Separation science and technology. Academic Press, pp 157–175

37. Caruso F, Mantellato S, Palacios M, Flatt RJ (2017) ICP-OES method for the characterization of cement pore solutions and their modification by polycarboxylate-based superplasticizers. Cem Concr Res 91:52–60. https://doi.org/10.1016/j.cemconres.2016.10.007

38. Khan SR, Sharma B, Chawla PA, Bhatia R (2022) Inductively coupled plasma optical emission spectrometry (ICP-OES): a powerful analytical technique for elemental analysis. Food Anal Methods 15:666–688. https://doi.org/10.1007/s12161-021-02148-4

39. Tyler G, Yvon J (1995) ICP-OES, ICP-MS and AAS techniques compared. ICP optical emission spectroscopy technical note 5

40. Wheal MS, Palmer LT (2010) Chloride analysis of botanical samples by ICP-OES. J Anal At Spectrom 25:1946–1952. https://doi.org/10.1039/C0JA00059K

41. Nunes TS, Muller CC, Balestrin P, Muller ALH, Mesko MF, Mello PdeA, Muller EI (2015) Determination of chlorine and sulfur in high purity flexible graphite using ion chromatography (IC) and inductively coupled plasma optical emission spectrometry (ICP OES) after pyrohydrolysis sample preparation. Anal Methods 7:2129–2134. https://doi.org/10.1039/C4AY02714K

42. Dietz T (2020) Quantifizierung von Chloriden in zementbasierten Feststoffen durch orts- und zeitaufgelöste Messung von Molekülemissionen in der laserinduzierten Plasmaspektroskopie

43. Houseaux J, Mermet J-M (2000) Use of a charge-coupled device detector in the 120–190 nm range in axially-viewed inductively coupled plasma atomic emission spectrometry. J Anal At Spectrom 15:979–982. https://doi.org/10.1039/B003626I

44. Luan S, Schleicher RG, Pilon MJ, Bulman FD, Coleman GN (2001) An echelle polychromator for inductively coupled plasma optical emission spectroscopy with vacuum ultraviolet wavelength coverage and charge injection device detection. Spectrochim Acta Part B 56:1143–1157. https://doi.org/10.1016/S0584-8547(01)00179-3

45. Pfaff JD, Hautman DP, Munch DJ (1997) Method 300.1 Determination of inorganic anions in drinking water by ion chromatography

46. Krämer D, Rosenberg E, Krug A, Kellner R, Hutter W, Hampel W (1994) Quantitative determination of chloride by means of flow injection analysis with spectrophotometric detection in the UV/VIS range. Mikrochim Acta 116:183–189. https://doi.org/10.1007/BF01260363

47. Watanabe A, Furukawa H, Miyamoto S, Minagawa H (2019) Non-destructive chemical analysis of water and chlorine content in cement paste using near-infrared spectroscopy. Constr Build Mater 196:95–104. https://doi.org/10.1016/j.conbuildmat.2018.11.114

48. Grahn W, Makedonski P, Wichern J, Kowalsky W, Wiese S (2002) Fiber optic sensors for an in-situ monitoring of moisture and pH value in reinforced concrete. In: imaging spectrometry VII. SPIE, pp 395–404

49. Bran-Anleu P, Caruso F, Wangler T, Pomjakushina E, Flatt RJ (2018) Standard and sample preparation for the micro XRF quantification of chlorides in hardened cement pastes. Microchem J 141:382–387. https://doi.org/10.1016/j.microc.2018.05.040

50. Dehghan A, Peterson K, Riehm G, Herzog Bromerchenkel L (2017) Application of X-ray microfluorescence for the determination of chloride diffusion coefficients in concrete chloride penetration experiments. Constr Build

Mater 148:85–95. https://doi.org/10.1016/j.conbuildmat.2017.05.072

51. Wilson W, Georget F, Scrivener KL (2024) Towards a two-step assessment of the chloride ingress behaviour of new cementitious binders. Cem Concr Res 184:107594. https://doi.org/10.1016/j.cemconres.2024.107594

52. Wilsch G, Weritz F, Schaurich D, Wiggenhauser H (2005) Determination of chloride content in concrete structures with laser-induced breakdown spectroscopy. Constr Build Mater 19:724–730. https://doi.org/10.1016/j.conbuildmat.2005.06.001

53. Millar S, Gottlieb C, Günther T, Sankat N, Wilsch G, Kruschwitz S (2018) Chlorine determination in cement-bound materials with laser-induced breakdown spectroscopy (LIBS)—a review and validation. Spectrochim Acta B At Spectrosc 147:1–8. https://doi.org/10.1016/j.sab.2018.05.015

54. Gehlen CD, Wiens E, Noll R, Wilsch G, Reichling K (2009) Chlorine detection in cement with laser-induced breakdown spectroscopy in the infrared and ultraviolet spectral range. Spectrochim Acta B At Spectrosc 64:1135–1140. https://doi.org/10.1016/j.sab.2009.07.021

55. Jakobsen UH, De Weerdt K, Geiker MR (2016) Elemental zonation in marine concrete. Cem Concr Res 85:12–27. https://doi.org/10.1016/j.cemconres.2016.02.006

56. Zibara H (2001) Binding of external chlorides by cement pastes. Thesis

57. Blunk G, Gunkel P, Srnolczyk H-G (1986) On the distribution of chloride between the hardening cement paste and its pore solution. 8th Int'l Cong Chem Cement 85–90

58. Byfors K (1986) Chloride binding in cement paste. Nordic Concr Res 27–38

59. Sandberg P, Larsson J (1993) Chloride binding in cement pastes in equilibrium with synthetic pore solutions. Chloride penetration into concrete structures, Nordic Miniseminar 98–107

60. Tang L, Nilsson L-O (1993) Chloride binding capacity and binding isotherms of OPC pastes and mortars. Cem Concr Res 23:247–253. https://doi.org/10.1016/0008-8846(93)90089-R

61. Hemstad P, Machner A, De Weerdt K (2020) The effect of artificial leaching with HCl on chloride binding in ordinary Portland cement paste. Cem Concr Res 130:105976. https://doi.org/10.1016/j.cemconres.2020.105976

62. Lothenbach B, Durdzinski P, De Weerdt K (2016) Thermogravimetric analysis. A practical guide to microstructural analysis of cementitious materials 1

63. Dhir RK, El-Mohr MAK, Dyer TD (1996) Chloride binding in GGBS concrete. Cem Concr Res 26:1767–1773. https://doi.org/10.1016/S0008-8846(96)00180-9

64. Glass GK, Wang Y, Buenfeld NR (1996) An investigation of experimental methods used to determine free and total chloride contents. Cem Concr Res 26:1443–1449. https://doi.org/10.1016/0008-8846(96)00115-9

65. Delagrave A, Marchand J, Ollivier J-P, Julien S, Hazrati K (1997) Chloride binding capacity of various hydrated cement paste systems. Adv Cem Based Mater 6:28–35. https://doi.org/10.1016/S1065-7355(97)90003-1

66. Truc O (2000) Prediction of chloride penetration into saturates concrete—multi-species approach. PhD Thesis

67. Glass GK, Buenfeld NR (1995) The determination of chloride binding relationships. In: Nilsson LO, Ollivier JP (eds) Chloride penetration into concrete, pp 36–42

68. Yuan Q, Shi C, De Schutter G, Audenaert K, Deng D (2009) Chloride binding of cement-based materials subjected to external chloride environment—a review. Constr Build Mater 23:1–13. https://doi.org/10.1016/j.conbuildmat.2008.02.004

69. Machner A, Bjørndal MH, Justnes H, Hanžič L, Šajna A, Gu Y, Bary B, Ben Haha M, Geiker MR, De Weerdt K (2022) Effect of leaching on the composition of hydration phases during chloride exposure of mortar. Cem Concr Res 153:106691. https://doi.org/10.1016/j.cemconres.2021.106691

70. Tritthart J (1989) Chloride binding in cement I. investigations to determine the composition of porewater in hardened cement. Cem Concr Res 19:586–594. https://doi.org/10.1016/0008-8846(89)90010-0

71. Jain A, Gencturk B, Pirbazari M, Dawood M, Belarbi A, Sohail MG, Kahraman R (2021) Influence of pH on chloride binding isotherms for cement paste and its components. Cem Concr Res 143:106378. https://doi.org/10.1016/j.cemconres.2021.106378

72. Mesbah A, Cau-dit-Coumes C, Frizon F, Leroux F, Ravaux J, Renaudin G (2011) A new investigation of the Cl^-–CO_3^2 substitution in AFm phases. J Am Ceram Soc 94:1901–1910. https://doi.org/10.1111/j.1551-2916.2010.04305.x

73. Angst U, Elsener B, Larsen CK, Vennesland Ø (2009) Critical chloride content in reinforced concrete—a review. Cem Concr Res 39:1122–1138. https://doi.org/10.1016/j.cemconres.2009.08.006

74. Angst UM, Elsener B, Larsen CK, Vennesland Ø (2011) Chloride induced reinforcement corrosion: electrochemical monitoring of initiation stage and chloride threshold values. Corros Sci 53:1451–1464. https://doi.org/10.1016/j.corsci.2011.01.025

75. Barneyback RS, Diamond S (1981) Expression and analysis of pore fluids from hardened cement pastes and mortars. Cem Concr Res 11:279–285. https://doi.org/10.1016/0008-8846(81)90069-7

76. Tuutti K (1982) Analysis of pore solution squeezed out of cement paste and mortar. Nordic Concr Res

77. Ramachandran VS, Seeley RC, Polomark GM (1984) Free and combined chloride in hydrating cement and cement components. Mater Constr 17:285–289. https://doi.org/10.1007/BF02479084

78. Haque MN, Kayyali OA (1995) Free and water soluble chloride in concrete. Cem Concr Res 25:531–542. https://doi.org/10.1016/0008-8846(95)00042-B

79. Castellote M, Andrade C (2001) Round-robin test on chloride analysis in concrete—part II: analysis of water soluble chloride content. Mater Struct 34:589–596. https://doi.org/10.1007/BF02482124

80. Arya C, Buenfeld NR, Newman JB (1987) Assessment of simple methods of determining the free chloride ion content of cement paste. Cem Concr Res 17:907–918. https://doi.org/10.1016/0008-8846(87)90079-2

81. Hope BB, Page JA, Poland JS (1985) The determination of the chloride content of concrete. Cem Concr

Res 15:863–870. https://doi.org/10.1016/0008-8846(85)90153-X

82. Chaussadent T, Arliguie G (1999) Afrem test procedures concerning chlorides in concrete: extraction and titration methods. Mat Struct 32:230–234. https://doi.org/10.1007/BF02481520

83. Ramachandran VS (1971) Possible states of chloride in the hydration of tricalcium silicate in the presence of calcium chloride. Mat Constr 4:3–12. https://doi.org/10.1007/BF02473926

84. Trejo D, Vaddey NP, Shakouri M (2019) Factors influencing chloride test results of cementitious systems. ACI Mater J 116:135–145. https://doi.org/10.14359/51712240

85. Ahmed AA, Trejo D (2023) Quantifying conservativeness of water-soluble chloride testing. ACI Mater J 120:13–24. https://doi.org/10.14359/51738499

86. Berman H (1972) Determination of chloride in hardened portland cement paste, mortar, and concrete. J Mater 330

87. ASTM (2004) ASTM C1556 Determination of the apparent chloride diffusion coefficient for hardened cementitious mixtures by bulk diffusion

88. Standards E BS EN 14629:2007 Products and systems for the protection and repair of concrete structures. Test methods. Determination of chloride content in hardened concrete

89. Sergi G, Yu SW, Page CL (1992) Diffusion of chloride and hydroxyl ions in cementitious materials exposed to a saline environment. Mag Concr Res 44:63–69. https://doi.org/10.1680/macr.1992.44.158.63

90. Georget F, Wilson W, Matschei T (2023) Long-term extrapolation of chloride ingress: an illustration of the feasibility and pitfalls of the square root law. Cem Concr Res 170:107187. https://doi.org/10.1016/j.cemconres.2023.107187

91. Crank J (1979) The mathematics of diffusion. Clarendon Press

92. Thomas JJ, Biernacki JJ, Bullard JW, Bishnoi S, Dolado JS, Scherer GW, Luttge A (2011) Modeling and simulation of cement hydration kinetics and microstructure development. Cem Concr Res 41:1257–1278. https://doi.org/10.1016/j.cemconres.2010.10.004

93. Hirao H, Yamada K, Takahashi H, Zibara H (2005) Chloride binding of cement estimated by binding isotherms of hydrates. J Adv Concr Technol 3:77–84. https://doi.org/10.3151/jact.3.77

94. Plusquellec G, Nonat A (2016) Interactions between calcium silicate hydrate (C–S–H) and calcium chloride, bromide and nitrate. Cem Concr Res 90:89–96. https://doi.org/10.1016/j.cemconres.2016.08.002

95. Beaudoin JJ, Ramachandran VS, Feldman RF (1990) Interaction of chloride and C–S–H. Cem Concr Res 20:875–883. https://doi.org/10.1016/0008-8846(90)90049-4

96. Harris M, Simpson G, Scrivener K, Bowen P (2022) A method for the reliable and reproducible precipitation of phase pure high Ca/Si ratio (> 1.5) synthetic calcium silicate hydrates (CSH). Cem Concr Res 151:106623. https://doi.org/10.1016/j.cemconres.2021.106623

97. Snellings R (2016) X-ray powder diffraction applied to cement. In: A practical guide to microstructural analysis of cementitious materials, 1st edn. CRC Press, p 70

98. Kouloumbi N, Batis G, Malami Ch (1994) The anticorrosive effect of fly ash, slag and a Greek pozzolan in reinforced concrete. Cem Concr Compos 16:253–260. https://doi.org/10.1016/0958-9465(94)90037-X

99. Luo R, Cai Y, Wang C, Huang X (2003) Study of chloride binding and diffusion in GGBS concrete. Cem Concr Res 33:1–7. https://doi.org/10.1016/S0008-8846(02)00712-3

100. Suryavanshi AK, Narayan Swamy R (1996) Stability of Friedel's salt in carbonated concrete structural elements. Cem Concr Res 26:729–741. https://doi.org/10.1016/S0008-8846(96)85010-1

101. Csizmadia J, Balázs G, Tamás FD (2001) Chloride ion binding capacity of aluminoferrites. Cem Concr Res 31:577–588. https://doi.org/10.1016/S0008-8846(01)00458-6

102. Goñi S, Guerrero A (2003) Accelerated carbonation of Friedel's salt in calcium aluminate cement paste. Cem Concr Res 33:21–26. https://doi.org/10.1016/S0008-8846(02)00910-9

103. Talero R, Trusilewicz L, Delgado A, Pedrajas C, Lannegrand R, Rahhal V, Mejía R, Delvasto S, Ramírez FA (2011) Comparative and semi-quantitative XRD analysis of Friedel's salt originating from pozzolan and Portland cement. Constr Build Mater 25:2370–2380. https://doi.org/10.1016/j.conbuildmat.2010.11.037

104. Talero R (2012) Synergic effect of Friedel's salt from pozzolan and from OPC co-precipitating in a chloride solution. Constr Build Mater 33:164–180. https://doi.org/10.1016/j.conbuildmat.2011.12.040

105. Ke X, Bernal SA, Provis JL (2017) Uptake of chloride and carbonate by Mg–Al and Ca–Al layered double hydroxides in simulated pore solutions of alkali-activated slag cement. Cem Concr Res 100:1–13. https://doi.org/10.1016/j.cemconres.2017.05.015

106. Li S, Jin Z, Yu Y (2021) Chloride binding by calcined layered double hydroxides and alumina-rich cementitious materials in mortar mixed with seawater and sea sand. Constr Build Mater 293:123493. https://doi.org/10.1016/j.conbuildmat.2021.123493

107. Paul G, Boccaleri E, Buzzi L, Canonico F, Gastaldi D (2015) Friedel's salt formation in sulfoaluminate cements: a combined XRD and ^{27}Al MAS NMR study. Cem Concr Res 67:93–102. https://doi.org/10.1016/j.cemconres.2014.08.004

108. Shi Z, Geiker MR, Weerdt KD, Østnor TA, Lothenbach B, Winnefeld F, Skibsted J (2017) Role of calcium on chloride binding in hydrated Portland cement–metakaolin–limestone blends. Cem Concr Res 95:205–216. https://doi.org/10.1016/j.cemconres.2017.02.003

109. Terzis A, Filippakis S, Kuzel H-J, Burzlaff H (1987) The crystal structure of $Ca_2Al(OH)_6Cl \cdot 2H_2O$. Zeitschrift für Kristallographie Cryst Mater 181:29–34. https://doi.org/10.1524/zkri.1987.181.14.29

110. Renaudin G, Kubel F, Rivera J-P, Francois M (1999) Structural phase transition and high temperature phase structure of Friedels salt, $3CaO \cdot Al_2O_3 \cdot CaCl_2 \cdot 10H_2O$.

Cem Concr Res 29:1937–1942. https://doi.org/10.1016/S0008-8846(99)00199-4

111. Jansen D, Goetz-Neunhoeffer F, Stabler C, Neubauer J (2011) A remastered external standard method applied to the quantification of early OPC hydration. Cem Concr Res 41:602–608. https://doi.org/10.1016/j.cemconres.2011.03.004

112. Avet F, Scrivener K (2020) Influence of pH on the chloride binding capacity of Limestone Calcined Clay Cements (LC3). Cem Concr Res 131:106031. https://doi.org/10.1016/j.cemconres.2020.106031

113. León-Reina L, De la Torre AG, Porras-Vázquez JM, Cruz M, Ordonez LM, Alcobé X, Gispert-Guirado F, Larrañaga-Varga A, Paul M, Fuellmann T, Schmidt R (2009) Round robin on Rietveld quantitative phase analysis of Portland cements. J Appl Crystallogr 42:906–916. https://doi.org/10.1107/S0021889809028374

114. Trník A, Scheinherrová L, Kulovaná T, Černý R (2016) Simultaneous differential scanning calorimetry and thermogravimetric analysis of Portland cement as a function of age. Int J Thermophys 37:12. https://doi.org/10.1007/s10765-015-2028-7

115. Gaviria X, Borrachero MV, Payá J, Monzó JM, Tobón JI (2018) Mineralogical evolution of cement pastes at early ages based on thermogravimetric analysis (TG). J Therm Anal Calorim 132:39–46. https://doi.org/10.1007/s10973-017-6905-0

116. DeJong MJ, Ulm F-J (2007) The nanogranular behavior of C–S–H at elevated temperatures (up to 700 °C). Cem Concr Res 37:1–12. https://doi.org/10.1016/j.cemconres.2006.09.006

117. Li C, Li J, Ren Q, Zhao Y, Jiang Z (2022) Degradation mechanism of blended cement pastes in sulfate-bearing environments under applied electric fields: sulfate attack vs. decalcification. Compos Part B Eng 246:110255. https://doi.org/10.1016/j.compositesb.2022.110255

118. Kim T, Olek J (2012) Effects of sample preparation and interpretation of thermogravimetric curves on calcium hydroxide in hydrated pastes and mortars. Transp Res Rec 2290:10–18. https://doi.org/10.3141/2290-02

119. Qiao C, Suraneni P, Nathalene Wei Ying T, Choudhary A, Weiss J (2019) Chloride binding of cement pastes with fly ash exposed to CaCl2 solutions at 5 and 23 °C. Cem Concr Compos 97:43–53. https://doi.org/10.1016/j.cemconcomp.2018.12.011

120. Suraneni P, Azad VJ, Isgor OB, Weiss J (2018) Role of supplementary cementitious material type in the mitigation of calcium oxychloride formation in cementitious pastes. J Mater Civ Eng 30:04018248. https://doi.org/10.1061/(ASCE)MT.1943-5533.0002425

121. Galan I, Perron L, Glasser FP (2015) Impact of chloride-rich environments on cement paste mineralogy. Cem Concr Res 68:174–183. https://doi.org/10.1016/j.cemconres.2014.10.017

122. Scrivener K, Bazzoni A, Berta M, Rossen JE (2016) Electron microscopy. In: Scrivener K, Snellings R, Lothenbach B (eds) A practical guide to microstructural analysis of cementitious materials. CRC Press

123. Goldstein J, Newbury DE, Joy DC, Lyman CE, Echlin P, Lifshin E, Sawyer L, Michael JR (2003) Scanning electron microscopy and X-ray microanalysis, 3rd edn. Springer

124. Bastin GF, Heijligers HJM (1990) Quantitative electron probe microanalysis of ultralight elements (boron-oxygen). Scanning 12:225–236. https://doi.org/10.1002/sca.4950120408

125. Georget F, Wilson W, Scrivener KL (2021) edxia: Microstructure characterisation from quantified SEM-EDS hypermaps. Cem Concr Res 141:106327. https://doi.org/10.1016/j.cemconres.2020.106327

126. Taylor HFW (1997) Cement chemistry. Thomas Telford

127. Harrisson AM, Winter NB, Taylor HFW (1987) X-ray microanalysis of microporous materials. J Mater Sci Lett 6:1339–1340. https://doi.org/10.1007/BF01794611

128. Thiery V, Dubois E, Bellayer S (2022) The good, the bad and the ugly polishing: effect of abrasive size on standardless EDS analysis of Portland cement clinker's calcium silicates. Micron. https://doi.org/10.1016/j.micron.2022.103266

129. Winnefeld F, Schöler A, Lothenbach B (2016) Sample preparation. In: Scrivener K, Snellings R, Lothenbach B (eds) A practical guide to microstructural analysis of cementitious materials. CRC Press

130. Plusquellec G, Geiker MR, Lindgård J, Duchesne J, Fournier B, De Weerdt K (2017) Determination of the pH and the free alkali metal content in the pore solution of concrete: review and experimental comparison. Cem Concr Res 96:13–26. https://doi.org/10.1016/j.cemconres.2017.03.002

131. De Weerdt K, Orsáková D, Geiker MR (2014) The impact of sulphate and magnesium on chloride binding in Portland cement paste. Cem Concr Res 65:30–40. https://doi.org/10.1016/j.cemconres.2014.07.007

132. De Weerdt K, Justnes H (2015) The effect of sea water on the phase assemblage of hydrated cement paste. Cem Concr Compos 55:215–222. https://doi.org/10.1016/j.cemconcomp.2014.09.006

133. De Weerdt K, Lothenbach B, Geiker MR (2019) Comparing chloride ingress from seawater and NaCl solution in Portland cement mortar. Cem Concr Res 115:80–89. https://doi.org/10.1016/j.cemconres.2018.09.014

134. De Weerdt K, Justnes H, Geiker MR (2014) Changes in the phase assemblage of concrete exposed to sea water. Cem Concr Compos 47:53–63. https://doi.org/10.1016/j.cemconcomp.2013.09.015

135. De Weerdt K, Orsáková D, Müller ACA, Larsen CK, Pedersen B, Geiker MR (2016) Towards the understanding of chloride profiles in marine exposed concrete, impact of leaching and moisture content. Constr Build Mater 120:418–431. https://doi.org/10.1016/j.conbuildmat.2016.05.069

136. Sandland TO, Du L-S, Stebbins JF, Webster JD (2004) Structure of Cl-containing silicate and aluminosilicate glasses: a 35Cl MAS-NMR study. Geochim Cosmochim Acta 68:5059–5069. https://doi.org/10.1016/j.gca.2004.07.017

137. Kirkpatrick RJ, Yu P, Hou X, Kim Y (1999) Interlayer structure, anion dynamics, and phase transitions in mixed-metal layered hydroxides: variable temperature 35Cl NMR spectroscopy of hydrotalcite and

Ca-aluminate hydrate (hydrocalumite). Am Mineral 84:1186–1190. https://doi.org/10.2138/am-1999-7-823

138. Baquerizo LG, Matschei T, Scrivener KL, Saeidpour M, Wadsö L (2015) Hydration states of AFm cement phases. Cem Concr Res 73:143–157. https://doi.org/10.1016/j.cemconres.2015.02.011

139. Barberon F, Baroghel-Bouny V, Zanni H, Bresson B, Caillerie J-B, Malosse L, Gan Z (2005) Interactions between chloride and cement-paste materials. Magn Reson Imaging 23:267–272. https://doi.org/10.1016/j.mri.2004.11.021

140. Yu P, Kirkpatrick RJ (2001) 35Cl NMR relaxation study of cement hydrate suspensions. Cem Concr Res 31:1479–1485. https://doi.org/10.1016/S0008-8846(01)00595-6

141. Cano FDJ, Bremner TW, McGregor RP, Balcom BJ (2002) Magnetic resonance imaging of 1 H, 23Na, and 35Cl penetration in Portland cement mortar. Cem Concr Res 32:1067–1070

142. Yun H, Patton ME, Garrett JJH, Fedder GK, Frederick KM, Hsu J-J, Lowe IJ, Oppenheim IJ, Sides PJ (2004) Detection of free chloride in concrete by NMR. Cem Concr Res 34:379–390

143. Ji Y, Pel L, Sun Z (2022) NMR study on the early-age hydration and ion binding of the cement paste prepared with NaCl solutions. Cem Concr Compos 129:104489. https://doi.org/10.1016/j.cemconcomp.2022.104489

144. Ji Y, Pel L, Zhang X, Sun Z (2021) Cl- and Na+ ions binding in slag and fly ash cement paste during early hydration as studied by 1H, 35Cl and 23Na NMR. Constr Build Mater 266:121606. https://doi.org/10.1016/j.conbuildmat.2020.121606

145. Jones MR, Macphee DE, Chudek JA, Hunter G, Lannegrand R, Talero R, Scrimgeour SN (2003) Studies using 27Al MAS NMR of AFm and AFt phases and the formation of Friedel's salt. Cem Concr Res 33:177–182. https://doi.org/10.1016/S0008-8846(02)00901-8

146. Peyvandi A, Holmes D, Balachandra AM, Soroushian P (2015) Quantitative analysis of chloride ion diffusion in cementitious materials using Al27 NMR spectroscopy. J Infrastruct Syst 21:04014047. https://doi.org/10.1061/(ASCE)IS.1943-555X.0000236

147. Lothenbach B, Winnefeld F (2006) Thermodynamic modelling of the hydration of Portland cement. Cem Concr Res 36:209–226. https://doi.org/10.1016/j.cemconres.2005.03.001

148. Lothenbach B (2010) Thermodynamic equilibrium calculations in cementitious systems. Mater Struct 43:1413–1433. https://doi.org/10.1617/s11527-010-9592-x

149. Loser R, Lothenbach B, Leemann A, Tuchschmid M (2010) Chloride resistance of concrete and its binding capacity—comparison between experimental results and thermodynamic modeling. Cem Concr Compos 32:34–42. https://doi.org/10.1016/j.cemconcomp.2009.08.001

150. Kulik D, Wagner T, Dmytrieva S, Kosakowski G, Hingerl F, Chudnenko K, Berner U (2013) GEM-selektor geochemical modeling package: revised algorithm and GEMS3K numerical kernel for coupled simulation codes. Comput Geosci 17:1–24. https://doi.org/10.1007/s10596-012-9310-6

151. Parkhurst DL, Appelo CAJ (2013) Description of input and examples for PHREEQC version 3—a computer program for speciation, batch-reaction, one-dimensional transport, and inverse geochemical calculations. In: U.S. Geological Survey Techniques and Methods. U.S. Geological Survey, p 497

152. Matschei T, Lothenbach B, Glasser FP (2007) Thermodynamic properties of Portland cement hydrates in the system CaO–Al$_2$O$_3$–SiO$_2$–CaSO$_4$–CaCO$_3$–H$_2$O. Cem Concr Res 37:1379–1410. https://doi.org/10.1016/j.cemconres.2007.06.002

153. Lothenbach B, Kulik DA, Matschei T, Balonis M, Baquerizo L, Dilnesa B, Miron GD, Myers RJ (2019) Cemdata18: a chemical thermodynamic database for hydrated Portland cements and alkali-activated materials. Cem Concr Res 115:472–506. https://doi.org/10.1016/j.cemconres.2018.04.018

154. Tran VQ, Soive A, Baroghel-Bouny V (2018) Modelisation of chloride reactive transport in concrete including thermodynamic equilibrium, kinetic control and surface complexation. Cem Concr Res 110:70–85. https://doi.org/10.1016/j.cemconres.2018.05.007

155. Glasser FP, Kindness A, Stronach SA (1999) Stability and solubility relationships in AFm phases: part I. Chloride, sulfate and hydroxide. Cem Concr Res 29:861–866

156. Samson E, Marchand J, Beaudoin JJ (2000) Modeling the influence of chemical reactions on the mechanisms of ionic transport in porous materials: an overview. Cem Concr Res 30:1895–1902. https://doi.org/10.1016/S0008-8846(00)00458-0

157. Matschei T, Lothenbach B, Glasser FP (2007) The role of calcium carbonate in cement hydration. Cem Concr Res 37:551–558. https://doi.org/10.1016/j.cemconres.2006.10.013

158. Hobbs MY (2001) Solubilities and ion exchange properties of solid solutions between the hydroxyl, chlorine and carbon trioxide end members of the monocalcium aluminate hydrates. UWSpace

159. Kari OP, Elakneswaran Y, Nawa T, Puttonen J (2013) A model for a long-term diffusion of multispecies in concrete based on ion–cement-hydrate interaction. J Mater Sci 48:4243–4259. https://doi.org/10.1007/s10853-013-7239-3

160. Yoshida S, Elakneswaran Y, Nawa T (2021) Electrostatic properties of C–S–H and C–A–S–H for predicting calcium and chloride adsorption. Cem Concr Compos 121:104109. https://doi.org/10.1016/j.cemconcomp.2021.104109